



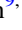




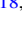
































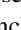



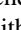
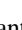









Publication Year	2022
Acceptance in OA	2022-03-22T14:19:25Z
Title	The Evolution of AGN Activity in Brightest Cluster Galaxies
Authors	Somboonpanyakul, T., McDonald, M., Noble, A., Agüena, M., Allam, S., Amon, A., Andrade-Oliveira, F., Bacon, D., Bayliss, M. B., Bertin, E., Bhargava, S., Brooks, D., Buckley-Geer, E., Burke, D. L., Calzadilla, M., Canning, R., Carnero Rosell, A., Carrasco Kind, M., Carretero, J., Costanzi, M., da Costa, L. N., Pereira, M. E. S., De Vicente, J., Doel, P., Eisenhardt, P., Everett, S., Evrard, A. E., Ferrero, I., Flaugher, B., Floyd, B., García-Bellido, J., Gaztanaga, E., Gerdes, D. W., Gonzalez, A., Gruen, D., Gruendl, R. A., Gschwend, J., Gupta, N., Gutierrez, G., Hinton, S. R., Hollowood, D. L., Honscheid, K., Hoyle, B., James, D. J., Jeltama, T., Khullar, G., Kim, K. J., Klein, M., Kuehn, K., Lima, M., Maia, M. A. G., Marshall, J. L., Martini, P., Melchior, P., Menanteau, F., Miquel, R., Mohr, J. J., Morgan, R., Ogando, R. L. C., Palmese, A., Paz-Chinchón, F., Pieres, A., Plazas Malagón, A. A., Reil, K., Romer, A. K., Ruppin, F., Sanchez, E., SARO, ALEXANDRO, Scarpine, V., Schubnell, M., Serrano, S., Sevilla-Noarbe, I., SINGH, PRIYANKA, Smith, M., Soares-Santos, M., STRAZZULLO, VERONICA, Suchyta, E., Swanson, M. E. C., Tarle, G., To, C., Tucker, D. L., Wilkinson, R. D.
Publisher's version (DOI)	10.3847/1538-3881/ac5030
Handle	http://hdl.handle.net/20.500.12386/31787
Journal	THE ASTRONOMICAL JOURNAL
Volume	163



The Evolution of AGN Activity in Brightest Cluster Galaxies

T. Somboonpanyakul^{1,2} , M. McDonald¹ , A. Noble³, M. Aguena⁴ , S. Allam⁵, A. Amon², F. Andrade-Oliveira^{4,6}, D. Bacon⁷, M. B. Bayliss⁸ , E. Bertin^{9,10} , S. Bhargava¹¹, D. Brooks¹² , E. Buckley-Geer^{5,13}, D. L. Burke^{2,14} , M. Calzadilla¹ , R. Canning¹⁵, A. Carnero Rosell^{4,16,17} , M. Carrasco Kind^{18,19} , J. Carretero²⁰ , M. Costanzi^{21,22,23} , L. N. da Costa^{4,24} , M. E. S. Pereira²⁵, J. De Vicente²⁶ , P. Doel¹², P. Eisenhardt²⁷, S. Everett²⁸, A. E. Evrard^{25,29} , I. Ferrero³⁰ , B. Flaugher⁵, B. Floyd³¹ , J. García-Bellido³² , E. Gaztanaga^{33,34} , D. W. Gerdes^{25,29} , A. Gonzalez³⁵ , D. Gruen³⁶ , R. A. Gruendl^{18,19} , J. Gschwend^{4,24} , N. Gupta³⁷ , G. Gutierrez⁵, S. R. Hinton³⁸ , D. L. Hollowood²⁸ , K. Honscheid^{39,40}, B. Hoyle³⁶, D. J. James⁴¹, T. Jeltema²⁸ , G. Khullar^{13,42} , K. J. Kim⁸ , M. Klein³⁶, K. Kuehn^{43,44} , M. Lima^{4,45}, M. A. G. Maia^{4,24}, J. L. Marshall⁴⁶ , P. Martini^{39,40,47}, P. Melchior⁴⁸ , F. Menanteau^{18,19} , R. Miquel^{20,49} , J. J. Mohr^{36,50}, R. Morgan⁵¹ , R. L. C. Ogando^{4,24} , A. Palmese^{5,42} , F. Paz-Chinchón^{18,19} , A. Pieres^{4,24} , A. A. Plazas Malagón⁴⁸ , K. Reil¹⁴, A. K. Romer¹¹ , F. Ruppin¹ , E. Sanchez²⁶ , A. Saro^{21,22,23,52}, V. Scarpine⁵, M. Schubnell²⁵, S. Serrano^{33,34} , I. Sevilla-Noarbe²⁶ , P. Singh^{22,23}, M. Smith⁵³ , M. Soares-Santos²⁵ , V. Strazzullo^{22,23,54} , E. Suchyta⁵⁵, M. E. C. Swanson¹⁸ , G. Tarle²⁵ , C. To^{2,14,56} , D. L. Tucker⁵ , and R. D. Wilkinson¹¹

¹ Kavli Institute for Astrophysics and Space Research, Massachusetts Institute of Technology, 77 Massachusetts Avenue, Cambridge, MA 02139, USA; taweevat@stanford.edu

² Kavli Institute for Particle Astrophysics & Cosmology, P.O. Box 2450, Stanford University, Stanford, CA 94305, USA

³ School of Earth and Space Exploration, Arizona State University, Tempe, AZ 85287, USA

⁴ Laboratório Interinstitucional de e-Astronomia—LIneA, Rua Gal. José Cristino 77, Rio de Janeiro, RJ—20921-400, Brazil

⁵ Fermi National Accelerator Laboratory, P. O. Box 500, Batavia, IL 60510, USA

⁶ Instituto de Física Teórica, Universidade Estadual Paulista, São Paulo, Brazil

⁷ Institute of Cosmology and Gravitation, University of Portsmouth, Portsmouth, PO1 3FX, UK

⁸ Department of Physics, University of Cincinnati, Cincinnati, OH 45221, USA

⁹ CNRS, UMR 7095, Institut d'Astrophysique de Paris, F-75014, Paris, France

¹⁰ Sorbonne Universités, UPMC Univ Paris 06, UMR 7095, Institut d'Astrophysique de Paris, F-75014, Paris, France

¹¹ Department of Physics and Astronomy, Pevsney Building, University of Sussex, Brighton, BN1 9QH, UK

¹² Department of Physics & Astronomy, University College London, Gower Street, London, WC1E 6BT, UK

¹³ Department of Astronomy and Astrophysics, University of Chicago, 5640 South Ellis Avenue, Chicago, IL 60637, USA

¹⁴ SLAC National Accelerator Laboratory, Menlo Park, CA 94025, USA

¹⁵ Institute of Cosmology and Gravitation, University of Portsmouth, PO1 2UP, UK

¹⁶ Instituto de Astrofísica de Canarias, E-38205 La Laguna, Tenerife, Spain

¹⁷ Universidad de La Laguna, Dpto. Astrofísica, E-38206 La Laguna, Tenerife, Spain

¹⁸ Center for Astrophysical Surveys, National Center for Supercomputing Applications, 1205 West Clark Street, Urbana, IL 61801, USA

¹⁹ Department of Astronomy, University of Illinois at Urbana-Champaign, 1002 West Green Street, Urbana, IL 61801, USA

²⁰ Institut de Física d'Altes Energies (IFAE), The Barcelona Institute of Science and Technology, Campus UAB, E-08193 Bellaterra (Barcelona), Spain

²¹ Astronomy Unit, Department of Physics, University of Trieste, via Tiepolo 11, I-34131 Trieste, Italy

²² Osservatorio Astronomico di Trieste, via G. B. Tiepolo 11, I-34143 Trieste, Italy

²³ Institute for Fundamental Physics of the Universe, Via Beirut 2, I-34014 Trieste, Italy

²⁴ Observatório Nacional, Rua Gal. José Cristino 77, Rio de Janeiro, RJ—20921-400, Brazil

²⁵ Department of Physics, University of Michigan, Ann Arbor, MI 48109, USA

²⁶ Centro de Investigaciones Energéticas, Medioambientales y Tecnológicas (CIEMAT), Madrid, Spain

²⁷ Jet Propulsion Laboratory, California Institute of Technology, 4800 Oak Grove Drive, M/S 169-327, Pasadena, CA 91109, USA

²⁸ Santa Cruz Institute for Particle Physics, Santa Cruz, CA 95064, USA

²⁹ Department of Astronomy, University of Michigan, Ann Arbor, MI 48109, USA

³⁰ Institute of Theoretical Astrophysics, University of Oslo, P.O. Box 1029 Blindern, NO-0315 Oslo, Norway

³¹ Department of Physics and Astronomy, University of Missouri—Kansas City, 5110 Rockhill Road, Kansas City, MO 64110, USA

³² Instituto de Física Teórica UAM/CSIC, Universidad Autónoma de Madrid, E-28049 Madrid, Spain

³³ Institut d'Estudis Espacials de Catalunya (IEEC), E-08034 Barcelona, Spain

³⁴ Institute of Space Sciences (ICE, CSIC), Campus UAB, Carrer de Can Magrans, s/n, E-08193 Barcelona, Spain

³⁵ Department of Astronomy, University of Florida, Gainesville, FL 32611, USA

³⁶ Faculty of Physics, Ludwig-Maximilians-Universität, Scheinerstrasse 1, D-81679 Munich, Germany

³⁷ CSIRO Astronomy & Space Science, PO Box 1130, Bentley, WA 6102, Australia

³⁸ School of Mathematics and Physics, University of Queensland, Brisbane, QLD 4072, Australia

³⁹ Department of Astronomy, The Ohio State University, Columbus, OH 43210, USA

⁴⁰ Center of Cosmology and Astro-Particle Physics, The Ohio State University, Columbus, OH 43210, USA

⁴¹ Center for Astrophysics | Harvard & Smithsonian, 60 Garden Street, Cambridge, MA 02138, USA

⁴² Kavli Institute for Cosmological Physics, University of Chicago, 5640 South Ellis Avenue, Chicago, IL 60637, USA

⁴³ Australian Astronomical Optics, Macquarie University, North Ryde, NSW 2113, Australia

⁴⁴ Lowell Observatory, 1400 Mars Hill Road, Flagstaff, AZ 86001, USA

⁴⁵ Departamento de Física Matemática, Instituto de Física, Universidade de São Paulo, CP 66318, São Paulo, SP, 05314-970, Brazil

⁴⁶ George P. and Cynthia Woods Mitchell Institute for Fundamental Physics and Astronomy, and Department of Physics and Astronomy, Texas A&M University, College Station, TX 77843, USA

⁴⁷ Radcliffe Institute for Advanced Study, Harvard University, Cambridge, MA 02138, USA

⁴⁸ Department of Astrophysical Sciences, Princeton University, Peyton Hall, Princeton, NJ 08544, USA

⁴⁹ Institució Catalana de Recerca i Estudis Avançats, E-08010 Barcelona, Spain

⁵⁰ Max Planck Institute for Extraterrestrial Physics, Giessenbachstrasse, D-85748 Garching, Germany

⁵¹ Physics Department, 2320 Chamberlin Hall, University of Wisconsin-Madison, 1150 University Avenue Madison, WI 53706-1390, USA

⁵² National Institute for Nuclear Physics, Via Valerio 2, I-34127 Trieste, Italy

⁵³ School of Physics and Astronomy, University of Southampton, Southampton, SO17 1BJ, UK

⁵⁴ Osservatorio Astronomico di Brera, Via Brera 28, I-20121 Milano, Italy⁵⁵ Computer Science and Mathematics Division, Oak Ridge National Laboratory, Oak Ridge, TN 37831, USA⁵⁶ Department of Physics, Stanford University, 382 Via Pueblo Mall, Stanford, CA 94305, USA

Received 2021 July 20; revised 2022 January 12; accepted 2022 January 13; published 2022 March 3

Abstract

We present the results of an analysis of Wide-field Infrared Survey Explorer (WISE) observations of the full 2500 deg² South Pole Telescope (SPT)-Sunyaev–Zel’dovich cluster sample. We describe a process for identifying active galactic nuclei (AGN) in brightest cluster galaxies (BCGs) based on WISE mid-IR color and redshift. Applying this technique to the BCGs of the SPT-SZ sample, we calculate the AGN-hosting BCG fraction, which is defined as the fraction of BCGs hosting bright central AGNs over all possible BCGs. Assuming an evolving single-burst stellar population model, we find statistically significant evidence (>99.9%) for a mid-IR excess at high redshift compared to low redshift, suggesting that the fraction of AGN-hosting BCGs increases with redshift over the range of $0 < z < 1.3$. The best-fit redshift trend of the AGN-hosting BCG fraction has the form $(1+z)^{4.1 \pm 1.0}$. These results are consistent with previous studies in galaxy clusters as well as in field galaxies. One way to explain this result is that member galaxies at high redshift tend to have more cold gas. While BCGs in nearby galaxy clusters grow mostly by dry mergers with cluster members, leading to no increase in AGN activity, BCGs at high redshift could primarily merge with gas-rich satellites, providing fuel for feeding AGNs. If this observed increase in AGN activity is linked to gas-rich mergers rather than ICM cooling, we would expect to see an increase in scatter in the P_{cav} versus L_{cool} relation at $z > 1$. Last, this work confirms that the runaway cooling phase, as predicted by the classical cooling-flow model, in the Phoenix cluster is extremely rare and most BCGs have low (relative to Eddington) black hole accretion rates.

Unified Astronomy Thesaurus concepts: [Galaxy clusters \(584\)](#); [Galaxy evolution \(594\)](#)

1. Introduction

Galaxy clusters are the most massive gravitationally bound and collapsed objects in the universe (Voit 2005). Because of their extremely deep potential wells, the temperature of the intracluster medium (ICM) is high enough to radiate X-rays. The central parts of clusters, which have the densest X-ray emitting gas, often have shorter cooling times than the Hubble time, implying that the hot X-ray gas should have had enough time to cool and form large inward flows of cooling material, known as cooling flows (Sarazin 1986; Fabian 1994). However, multiwavelength observations have only seen a fraction of the massive cooling flows that are expected from standard cooling models (e.g., O’Dea et al. 2008; Donahue et al. 2015; McDonald et al. 2018). This is referred to as “the cooling-flow problem,” and active galactic nucleus (AGN) feedback is thought to be responsible for preventing the hot gas from cooling by propagating energy from the supermassive black hole (SMBH) to the ICM. The two primary modes of AGN feedback are the kinetic mode, in which relativistic jets push the hot gas aside and create cavities, and the quasar mode, in which the radiation comes from the accretion disk (see reviews by Fabian 2012; McNamara & Nulsen 2012).

With the recent development of galaxy cluster surveys that use the Sunyaev–Zel’dovich (SZ) effect (Sunyaev & Zeldovich 1972), such as the South Pole Telescope (SPT; Carlstrom et al. 2011; Bleem et al. 2015, 2020; Huang et al. 2020) and the Atacama Cosmology Telescope (ACT; Hilton et al. 2018, 2021), the number of known high- z ($z > 1$) clusters with good mass estimates has increased dramatically. This has enabled many studies of the evolution of AGN feedback in clusters over cosmic time (McDonald et al. 2013, 2017; Gupta et al. 2020). However, the evolution of AGN feedback in galaxy clusters

with redshift remains poorly understood. In particular, Hlavacek-Larrondo et al. (2015) found no evidence for evolution in jetted power generated by AGN feedback from X-ray cavities over the past 7 Gyr ($z = 0.8$). An earlier study by Hlavacek-Larrondo et al. (2013) suggested that the fraction of brightest cluster galaxies (BCGs) with X-ray bright nuclei is decreasing with time (or increasing with redshift), suggesting a strong evolution in radiative mode feedback. In contrast, a recent study looking for nuclear BCG X-ray emission in Chandra archival data instead found no evidence for an evolution between two redshift bins ($\langle z \rangle \sim 0.25$ and $\langle z \rangle \sim 0.65$; Yang et al. 2018). The disagreement between various studies about the evolution of the AGN feedback restricts our ability to fully understand this issue.

In this work, we calculate the AGN-hosting BCG fraction by identifying BCGs in the 2500 deg² SPT-SZ cluster samples (Bleem et al. 2015) and by classifying whether they are AGNs based on mid-IR data. The SZ cluster catalogs allow for an effectively mass-selected sample of clusters, making it possible to study the evolution of galaxy clusters over time. In addition, the SZ catalogs typically have less contamination compared to optical/IR catalogs. The fraction of BCGs hosting luminous AGNs is an important indicator for AGN fueling processes, availability of cold clumpy gas in the centers of clusters, the duration and duty cycle of the AGNs, and how BCGs and the host clusters grow and evolve together. This is because additional physical mechanisms are often required to explain the transport of the cold gas, which serves as the primary fuel source for the central black holes. The fact that we find a relative absence of AGNs in the centers of clusters has led us to study many physical processes, including ram pressure stripping (Gunn & Gott 1972), tidal effects from the cluster gravitational potential (Merritt 1983), and the lack of new infall of cold gas (Larson et al. 1980). Similarly, understanding the evolution of AGN activities in BCGs will help us understand the evolution mechanism of galaxy clusters, and how the feedback might play a role in it.



Original content from this work may be used under the terms of the [Creative Commons Attribution 4.0 licence](#). Any further distribution of this work must maintain attribution to the author(s) and the title of the work, journal citation and DOI.

Our goal for this paper is to study the redshift evolution of the AGN-hosting BCG fraction up to $z = 1.3$ to understand the fueling processes in the centers of clusters, determine when AGN feedback is fully established, and identify whether there are any more extreme AGN-hosting BCGs in the sample, similar to the Phoenix cluster. The paper is organized as follows. In Sections 2 and 3 we summarize the data and additional information used in this paper. The results and their implications are presented in Sections 4 and 5, respectively. We conclude our work in Section 6. We assume $H_0 = 70 \text{ km s}^{-1} \text{ Mpc}^{-1}$, $\Omega_m = 0.3$ and $\Omega_\lambda = 0.7$. All errors are 1σ unless noted otherwise.

2. Data

2.1. The SPT-SZ 2500 deg² Cluster Sample

We use the full 2500 deg² SPT-SZ cluster sample from Bleem et al. (2015) with the improvement in the cluster redshift estimates from Bocquet et al. (2019) by incorporating new spectroscopic and improved photometric measurements (Bayliss et al. 2016; Khullar et al. 2019). The survey spans a contiguous 2500 deg² area within a boundary of R.A. = 20 hr–7 hr and decl. = -65° to -40° . Once we limit the redshift range to $0 < z < 1.3$, the total number of clusters in our sample is 475.

2.2. Position of BCGs

Given the diversity of BCG colors, morphologies, and assembly state as a function of redshift, typical identification algorithms may be biased when they select BCGs based on single-band fluxes. We have instead developed a novel BCG identification pipeline that uses the full probability distribution of redshift and stellar mass for every object within 500 projected kiloparsec of the SZ cluster center to assign BCG likelihoods. Photometry is provided by the Dark Energy Survey (Year 3) catalogs (Jarvis et al. 2021; Sevilla-Noarbe et al. 2021), cross-correlated with unWISE (Lang 2014), which is a combination of WISE and NEOWISE images. Various cuts and flags are used to avoid stars and objects with poor photometric measurements. WISE is an IR-wavelength space satellite with four IR filters, including W1 ($\lambda_{cen} = 3.6 \mu\text{m}$), W2 ($4.3 \mu\text{m}$), W3 ($12 \mu\text{m}$), and W4 ($22 \mu\text{m}$; Wright et al. 2010). The satellite operated for two years with cryogen until 2011, before it was reactivated and resumed operations as NEOWISE in 2013. It has continued to observe ever since (Mainzer et al. 2014).

Probability distributions of photometric redshift and stellar mass for each source are estimated with EAZY (Brammer et al. 2008) and FAST (Kriek et al. 2009), respectively. We then randomly sample from each distribution to find the most massive cluster galaxy at the cluster redshift within each field, iterating this process 10^5 times to build up a BCG likelihood for each galaxy. In this way, all galaxies are assigned a value between 0% and 100% probability of being the BCG within each cluster. Full details about the pipeline, along with the BCG catalog, will be provided in Noble et al. (in preparation). The top three panels of Figure 1 show optical images of example SPT galaxy clusters with identified BCGs in white squares. This demonstrates that the algorithm selects likely BCGs that match the galaxies that typical or traditional visual BCG identification methods would select over a wide range of redshift.

2.3. Data for AGN Selection

Most photometric techniques for identifying AGNs are severely biased toward unobscured (type 1) AGNs since their nuclear emissions dominate the emission of the host galaxies, making these AGNs easily identifiable. This implies that most obscured (type 2) AGNs are often underrepresented in most studies. The most promising techniques for identifying both obscured and unobscured AGNs include radio, hard X-ray, and mid-IR selections. However, not all AGNs are radio loud (e.g., Stern et al. 2000), and the current hard X-ray satellites remain limited in their sensitivity and field of view. This leaves mid-IR selection as a popular technique to quickly identify large AGN populations (obscured and unobscured). The idea of mid-IR selection is to separate between the power-law AGN spectrum and the blackbody stellar spectrum of galaxies, which peaks at rest frame $1.6 \mu\text{m}$. The power-law spectra of the AGNs are due to the thermal emission from the warm-hot dust in the torus, which is heated by absorbing shorter-wavelength photons from the accretion disk (Stern et al. 2012; Hickox & Alexander 2018). This implies that the emission is not strongly suppressed by the dusty torus, unlike at the UV to near-IR wavelength, allowing this technique to detect more obscured AGNs. Additionally, with the first all-sky data release of the Wide-field Infrared Survey Explorer (WISE; Wright et al. 2010) in 2012, mid-IR selection became one of the top methods of probing the AGN population over the entire sky without additional observations.

One drawback of the mid-IR selection technique is that the host galaxy is still bright at these wavelengths, limiting the detection of low-luminosity AGN, which have to compete with a bright stellar continuum (Stern et al. 2012). This means that AGNs that are selected by their mid-IR color tend to be brighter relative to the host galaxies than those selected by other techniques. For example, Assef et al. (2013) found that in the sample of relatively luminous AGNs ($L_{\text{AGN}}/L_{\text{host}} > 0.5$), the luminosity of mid-IR AGNs tends to be greater than $\sim 5 \times 10^{44} \text{ erg s}^{-1}$, taking into account the bolometric correction from Singal et al. (2016). Assuming the efficiency of turning accreting matter into energy $\epsilon_{\text{acc}} = 0.1$ and a typical mass of the SMBH $M_{\text{BH}} \sim 10^8 - 10^9 M_\odot$ (Russell et al. 2013), the black hole mean accretion rate ($\dot{M}_{\text{BH}} = L_{\text{bol,nuc}}/\epsilon_{\text{acc}} c^2$) of mid-IR selected AGNs should be greater than $4 \times 10^{-3} - 4 \times 10^{-2} \dot{M}_{\text{Edd}}$, where \dot{M}_{Edd} is the limiting Eddington accretion rate. This level of accretion is relatively high compared to typical optical/radio AGNs, which have an accretion rate of about $10^{-6} - 10^{-2} \dot{M}_{\text{Edd}}$ (McDonald et al. 2021). This implies that the mid-IR technique will mainly identify a brighter and more massive AGN population. From now on, AGNs mentioned in this paper mean the mid-IR selected AGN population.

2.3.1. Mid-infrared Data from WISE

Instead of using the main source catalog from WISE (AllWISE), which only includes the data obtained from 2010 to 2011, we make use of CatWISE to obtain the best photometry with available data. CatWISE is an updated all-sky IR source catalog that combines the 2010 and 2011 data from WISE with the 2013 through 2016 NEOWISE data (Eisenhardt et al. 2020). The caveat is that the CatWISE catalog only includes 3.6 (W1) and 4.3 (W2) μm data. In this work, we use the Preliminary CatWISE catalog to obtain the